Molecular Human Reproduction, pp. 1–12, 2022
https://doi.org/10.1093/molehr/gaac029

molecular human reproduction

ORIGINAL RESEARCH

Sperm degradation after vasectomy follows a sperm chromatin fragmentation-dependent mechanism causing DNA breaks in the toroid linker regions

Jordi Ribas-Maynou [1,2,3,*], Hieu Nguyen [3], Raquel Valle [3], Hongwen Wu [3], Marc Yeste [1,2,4], and W. Steven Ward [3,5]

[1]Unit of Cell Biology, Department of Biology, Faculty of Sciences, University of Girona, Girona, Spain [2]Biotechnology of Animal and Human Reproduction (TechnoSperm), Institute of Food and Agricultural Technology, University of Girona, Girona, Spain [3]Department of Anatomy, Biochemistry and Physiology, Institute for Biogenesis Research, John A. Burns School of Medicine, University of Hawaii at Manoa, Honolulu, HI, USA [4]Catalan Institution for Research and Advanced Studies (ICREA), Barcelona, Spain [5]Department of Obstetrics, Gynecology & Women's Health, John A. Burns School of Medicine, University of Hawaii at Manoa, Honolulu, HI, USA

*Correspondence address. Unit of Cell Biology, Department of Biology, Faculty of Sciences, University of Girona, 69 Maria Aurèlia Campmany, 17003 Girona, Spain. Tel: +34-972-419514; Fax: +34-972-41150; E-mail: jordi.ribasmaynou@udg.edu https://orcid.org/0000-0002-9101-2044

Submitted on May 24, 2022; resubmitted on July 14, 2022; editorial decision on August 1, 2022

ABSTRACT: Vasectomy is a widely used surgical technique creating an obstructive azoospermia. Although sperm cannot be ejaculated, the testis maintains sperm production in vasectomized males. The continuous accumulation of sperm deposited in the epididymis and the vas deferens fraction necessarily need to be degraded and eliminated. While the elimination process is carried out by granulomas that form after vasectomy, the detailed mechanisms of sperm degradation are still not known. The aim was to assess whether sperm chromatin fragmentation (SCF), a mechanism that degrades the entire sperm genome at the toroid linker regions (TLRs), is activated after vasectomy in sperm cells. We vasectomized mice and evaluated the presence of TLR-specific double-strand breaks through pulsed-field gel electrophoresis and the Comet assay at 1, 2 and 3 weeks after surgery. Results for DNA damage (Olive tail moment) at single-cell level showed an increase of double-strand breaks after vasectomy for vas deferens sperm after 1, 2 and 3 weeks postvasectomy (21.78 ± 2.29; 19.71 ± 1.79 and 32.59 ± 1.81, respectively), compared to mock surgery (7.04 ± 1.03; 10.10 ± 1.29 and 8.64 ± 0.85, respectively; $P < 0.001$). Similar findings were obtained for cauda epididymis sperm ($P < 0.001$), but not for caput epididymis ($P > 0.05$). Pulsed-field gel electrophoresis showed the presence of double-stranded breaks between 15 and 145 kb, indicating that DNA breaks were produced mainly in the sperm TLRs. Results presented here suggest that SCF is a mechanism activated in vas deferens after vasectomy to degrade sperm DNA when they cannot be ejaculated, preventing their function.

Key words: vasectomy / sperm degradation / sperm chromatin fragmentation / DNA damage / vas deferens / epididymis

Introduction

During spermatogenesis, sperm chromatin is remodeled into a highly condensed state by protamines and only retains a small percentage of histones, ranging from <1% to 15% depending on the mammalian species (Mudrak *et al.*, 2005; Hammoud *et al.*, 2009; Samans *et al.*, 2014; Mendonça *et al.*, 2017). Protamines organize DNA into toroidal structures (Hud *et al.*, 1995), which condense roughly 25–50 kb of DNA and are linked together and attached to the nuclear scaffold by the toroid linker regions (TLRs) (Ward, 2010). This leads to a highly condensed nucleus, which functions to protect the paternal genome from genotoxic agents during its transit toward the oocyte. This protection, however, is not totally effective since sperm with fragmented DNA are often observed after ejaculation, with different incidences among species (Castro *et al.*, 2018; Peris-Frau *et al.*, 2019; Crespo *et al.*, 2020; Ribas-Maynou *et al.*, 2021; Esteves *et al.*, 2022). *In vitro* experiments, which attempted to actively damage sperm DNA, have shown that sperm chromatin limits chromatin breaks caused by nucleases to the TLRs (Sotolongo *et al.*, 2003), while damage caused by reactive oxygen species may affect both toroidal regions and TLRs, thus

leading to a more localized damage when double-strand breaks (DSBs) are produced by enzymes, and more extensive damage when DNA is oxidized (Villani et al., 2010; Ribas-Maynou and Benet, 2019).

Despite the highly condensed nucleus, previous studies had shown that sperm cells may retain certain functional aspects that are inherent to their structure. For instance, it has been demonstrated that decondensed sperm DNA (sperm haloes) having extracted histones and protamines retain their ability to fertilize oocytes and produce normal chromosomes, and their ability to support DNA replication (Mohar et al., 2002; Shaman et al., 2007). Importantly, we have also found that sperm have the ability to partially degrade their DNA *in vitro* upon incubation with Mn^{2+}, by a mechanism we term sperm chromatin fragmentation (SCF). The SCF causes the specific breakage at TLR regions, leading to a toroid-size break pattern when visualized by pulsed-field gel electrophoresis (PFGE) (Sotolongo et al., 2005; Boaz et al., 2008). The effects of the activation of a nuclease in mature sperm cells may resemble the activity of nucleases that takes place during the apoptotic process in somatic cells, leading to a pattern of fragments of regular sizes (Gong et al., 1994; Solovyan et al., 2002). The SCF in mature sperm degrades only the most accessible chromatin domains and can prevent embryo development (Gawecka et al., 2013). Previous research supports the presence of an extracellular nuclease located either inside or outside membrane-covered vesicles that causes the DNA degradation in SCF, which may reach nuclear DNA directly through damaged membranes or vesicle internalization and exert DNA damage (Gawecka, 2015). Our evidence, however, still does not rule out the possibility that SCF activity could be driven by a topoisomerase II that may remain attached to the nuclear matrix at the TLR region (Yamauchi et al., 2007b). In fact, using the Comet assay, we have shown that DSBs caused by SCF remain attached to the nuclear matrix at the early stages of SCF, thus providing an opportunity to be repaired after fertilization, which may indicate that a protein, such as a topoisomerase, could be implicated in this attachment (Ribas-Maynou et al., 2014).

Vasectomy is a surgical procedure where sperm ejaculation is completely obstructed by physically interrupting the vas deferens. Research assessing the effects of vasectomy reported that the interruption of sperm transit through the vas deferens does not cause a rapid decrease of epididymis and testicular sperm function (Borges et al., 2003; Peng et al., 2008), and some authors suggested that the effects of vasectomy on the sperm's fertilization ability using ICSI is maintained, even 15 years after vasectomy (Borges et al., 2019). Yet, different reports demonstrated that the presence of testicular sperm and their capacity to fertilize an oocyte are reduced in a time-dependent manner after vasectomy (Bedford and Zelikovsky, 1979; Richardson et al., 1984; Abdelmassih et al., 2002; Borges et al., 2003, 2019). In fact, several attrition effects impairing sperm generation or maturation have been published, such as an increased p53 and germ cell apoptosis (Shiraishi et al., 2001, 2002), a drop in intact sperm cells thereby increasing the presence of isolated heads or tails (Khaira et al., 2007), alterations in the transcription pattern of different genes at the epididymal epithelia (Doiron et al., 2003; Légaré et al., 2004; Belleannée et al., 2013) and the appearance of DNA breaks and apoptotic markers in epididymal and testicular sperm (Ramos et al., 2004; O'Neill et al., 2007; Hammoud et al., 2017). Since vasectomy does not stop sperm production but prevents their ejaculation, sperm cells need to be degraded and removed from the reproductive tract. It is known that vasectomy causes a distension of the epididymis duct, generating a higher pressure that promotes the appearance of a granuloma, which is believed to be part of the sperm elimination mechanism (Nashan et al., 1990; Sun et al., 1992; Jessop and Ladds, 1995), but the precise mechanisms driving sperm degradation are still unknown. These data support our hypothesis that SCF, a mechanism heretofore seen only *in vitro*, causes sperm DNA degradation after vasectomy, *in vivo*.

Materials and methods

Reagents

Unless otherwise stated, the reagents used for the present work were purchased from Sigma-Aldrich (St. Louis, MO, USA).

Animals, vasectomy procedure and sperm collection

For all experiments, B6 (C57BL) mice were used. Mice were obtained from Jackson Laboratory (Bar Harbor, ME, USA) and were maintained until 8–10 weeks of age in standard cages containing five or less mice per cage, with standard food and water *ad libitum*. The procedures for animal handling were reviewed and approved by the Institutional Animal Care and Use Committee of the University of Hawaii (Protocol number 04-049-18).

Vasectomy was conducted in 8- to 9-week-old males. First, mice were anesthetized by i.p. injection with 0.25–0.5 mg/g of aventin. A ventral incision was made to access a vas deferens, which was pulled out from the abdominal cavity. At that point, an end cut was made to the vas deferens, and it was immediately returned to the abdominal cavity. The same procedure was repeated with the other vas deferens. Finally, the skin was sutured and held with wound clips. Mice were allowed to recover from anesthesia in their cages and were periodically checked to ensure that the wound had healed. Control mice were produced through mock surgery, which was conducted following the same procedure as vasectomy but avoiding the end cut to the vas deferens.

For sperm collection, animals were euthanized with the cervical dislocation procedure. The epididymis and vas deferens were then dissected and sperm were retrieved from caput epididymis, cauda epididymis and vas deferens. Unless otherwise stated, sperm were diluted in 25 mM Tris–HCl, pH 8, supplemented with 0.25% Triton X-100.

In vitro SCF treatment

Briefly, sperm cells from both epididymis and vas deferens were collected in 20 mM Tris–HCl, 0.25% Triton X-100, pH 7.5 and then treated with 10 mM $MnCl_2$, for 30 min at 37°C. Following this, 50 mM EDTA was added, and the mixture was incubated for a further 30 min at 37°C. Control sperm were first incubated for 30 min without the addition of $MnCl_2$ and then incubated for 30 min with 50 mM EDTA at 37°C. Both samples were used for the corresponding experiment using the appropriate method described below.

Viability assay

For the viability assay, sperm were collected in human tubal fluid media (Life Global, Cooper Surgical, Trumbull, CT, USA) and mixed

gently. Subsequently, 5 µl of sperm was placed onto a microscopy slide and mixed with 5 µl of 1% eosin. Finally, the sample was covered with a coverslip and evaluated under bright field in an Olympus BX51 microscope (Tokyo, Japan). One hundred sperm cells were assessed and classified as viable (white colored) or non-viable (dark-pink colored). The percentage of live sperm was recorded.

Pulsed-field gel electrophoresis

First, sperm samples were concentrated to 300 million sperm/ml, and they were prewarmed at 38°C and mixed 1:1 (v:v) with 2% low melting point agarose at 38°C. Immediately after, the mixture was poured into CHEF plug molds (BioRad, Hercules, USA) and allowed to jellify at 4°C for 15 min. Once the plugs had solidified, they were placed in digestion buffer (10 mM Tris–HCl, 10 mM EDTA, 100 mM NaCl, 20 mM dithiothreitol (DTT), 2% sodium dodecyl sulfate (SDS) and 20 mg/ml proteinase K, pH 8.0) for 60 min at 53°C. Meanwhile, a 1% pulsed-field agarose gel in 0.5× Tris/borate/EDTA buffer (TBE; 0.445 M Tris–HCl, 0.445 M Boric acid and 0.01 M EDTA, pH 8), containing 1 µg/ml ethidium bromide, was cast in a gel tray. Afterward, plugs were placed into the wells of the pulsed-field gel and it was run on a contour-clamped homogeneous electric field apparatus (CHEF-DR III Variable Angle System, BioRad, Hercules, CA, USA) in circulating 0.5× TBE buffer at 14°C, for 16 h. The pulsed-field protocol was set to the autoalignment algorithm for a molecular weight range of 5–200 kb, which included an electrode angle change of 120° with an initial switch time of 1 s and the final switch time of 25 s. The MidRange PFG Marker (15–291 kb; New England Biolabs, Ipswich, MA, USA) was included in each gel for molecular weight reference. After electrophoresis was complete, the gel was imaged in an LAS-3000 gel imager (Fujifilm, Tokyo, Japan), avoiding overexposure (1 s of exposure time).

DNA fragment quantification

The Image Studio Lite (LI-COR Biosciences, Lincoln, NE, USA) was used to quantify the intensity of each lane, and taking into account the DNA ladder. The percentages of fragmented DNA with fragments between 15 and 145 kb, corresponding to the size condensed in a sperm toroid, were recorded.

Neutral and alkaline Comet assay

The Comet assay was performed in neutral pH conditions for the detection of double-stranded DNA breaks, and in alkaline denaturing conditions for the detection of global DNA damage. The protocol used is separated into different stages, as described below.

Sperm-agarose mixture and lysis

First, sperm were diluted to a concentration of 1×10^6 sperm/ml and warmed to 38°C. Then, an aliquot of 1.5% low melting point agarose was melted at 80°C and cooled to 38°C. Once 38°C was reached, sperm and agarose were mixed in 1:2 (v:v) proportion, leading to a final concentration of 1% low melting point agarose. Thereafter, 10 µl of the mixture was placed on top of two agarose pretreated slides, one for the neutral Comet assay and the other for the alkaline Comet assay, covered with two 8-mm diameter coverslips and allowed to jellify at 4°C for 1 min on a metal plate. The coverslips were then gently removed and both slides were incubated in two lysis solutions for 30 min each. The first lysis solution contained 0.8 M Tris–HCl, 0.8 M DTT and 1% SDS (pH 7.5) and the second contained 0.4 M Tris–HCl, 0.4 M DTT, 50 mM EDTA and 2 M NaCl (pH 7.5). After lysis, sperm were washed in 20 mM Tris–HCl, pH 7.5 for 5 min.

Electrophoresis

For the neutral Comet, electrophoresis was performed at 1 V/cm for 4 min in TBE buffer, and then the slide was washed in 0.9% NaCl solution for 2 min. For the alkaline Comet, the slide was incubated in a denaturing alkaline solution (0.03 M NaOH, 1 M NaCl) for 5 min at 4°C, and electrophoresis was conducted at 1 V/cm for 4 min in NaOH buffer (0.03 M NaOH, pH 13).

Neutralization, dehydration and staining

Both neutral and alkaline slides were incubated in a neutral pH solution (0.4 M Tris–HCl, pH 7.5) for 5 min at room temperature, dehydrated in 70%, 90% and 100% ethanol for 2 min each, and allowed to dry horizontally. After drying, both slides were stained through incubation in 1× SYBR Safe DNA Gel Stain (ThermoFisher Scientific, Waltham, MA, USA) for 15 min, followed by washing in dH_2O for 3 min and allowed to dry.

Imaging

An Olympus BX51 epifluorescence microscope (Tokyo, Japan), using the FITC filter was used to visualize Comets. At least 100 sperm cells per sample were captured using the CellSens software (Olympus, Tokyo, Japan) coupled to an Olympus DP80 Dual-Sensor camera. For each capture, the exposure time was adapted to avoid overexposure of any Comet region and images were obtained in 14-bit monochrome format with a resolution of 1916 × 912 pixels.

Analysis of Comet images

Analysis of the Comet images was conducted using the open-access CometScore v2.0 software (Rexhoover, http://rexhoover.com/cometscoredownload.php), which quantifies the fluorescence of the Comet heads and tails. Images were automatically evaluated, adjusting the background intensity to correctly visualize the Comets. However, after the automatic analysis, a manual review of each Comet was conducted in order to remove overlapping Comets, eliminate captures not corresponding to Comets and correct head and tail detection for misanalyzed Comets. If the final number of Comets was <50, more pictures were captured under the microscope until the number of correctly analyzed Comets reached this figure.

Olive tail moment (OTM) was chosen as an indicator of the amount of DNA breaks present in a specific cell, as it has been shown to be the most informative parameter (Langie *et al.*, 2015; Simon *et al.*, 2017). OTM is defined by the following formula: (tail mean intensity − head mean intensity) × Tail DNA/100. Tail DNA is defined as the percentage of DNA that moved to the Comet tail after electrophoresis.

Somatic cell lysis for caput sperm analysis

Sperm retrieval from the caput epididymis requires the disaggregation of the entire caput, which means that the sample containing sperm also includes contaminating somatic cells. In order to assess the DNA damage affecting sperm cells, caput samples were incubated in cell lysis solution (10 mM Tris–HCl, 1% Triton X-100, 5% SDS, 100 mM EDTA and pH 7.5) for 10 min at room temperature, vortexing for 10 s every 3 min. To set up the methodology, we treated caput sperm with the

somatic cell lysis solution described above and we assessed whether there was a change in DNA fragmentation after the treatment. Results were compared with cauda epididymis sperm, which are not contaminated with somatic cell lysis during their retrieval. Imaging under a fluorescence microscope was conducted after staining with 1× SYBR Safe DNA Gel Stain (ThermoFisher Scientific, Waltham, MA, USA) for 15 min to evaluate the presence of somatic cells.

Transmission electron microscopy

Sperm were first fixed in 2.5% glutaraldehyde in 0.1 M sodium cacodylate buffer, at pH 7.4, for 2 h at room temperature. After fixation, sperm were washed three times in 0.1 M sodium cacodylate buffer for 30 min. Thereafter, samples were postfixed with 1% osmium tetroxide in 0.1 M sodium cacodylate buffer for 1 h and dehydrated in a graded ethanol series (30%, 50%, 70%, 80% and 95%) for 5 min each. Samples were subsequently incubated in 100% ethanol for 10 min. Once dehydrated, samples were infiltrated with propylene oxide and epoxy resin (1:1) overnight. On the next day, samples were immersed in freshly prepared 100% epoxy resin for 8 h, with two changes to fresh epoxy resin every 2–3 h. Finally, samples were placed in molds with 100% epoxy resin and allowed to polymerize at 60°C for 2–3 days. Ultrathin sections (60–80 nm) were obtained using an RMC Powertome ultramicrotome (Boeckeler Instruments, Tucson, AZ, USA), which were stained with 2% uranyl acetate/0.3% lead citrate. Samples were visualized under a Hitachi HT7700 transmission electron microscope (Hitachi, Tokyo, Japan) at 10 000× magnification and 100 kV and photographed with an AMT BioSprint16 camera (AMT Imaging, Woburn, MA, USA) taking 10 drift frames at 320 ms at a resolution of 4896 × 3920 pixels.

Statistical analysis

Data were analyzed with the GraphPad Prism 8.0 Software (GraphPad, San Diego, CA, USA), and graphs were compiled with the same software. First, data were checked for their fit with a normal distribution and the homogeneity of variances using the Shapiro–Wilk and Levene tests, respectively. Because data did not fit with parametric assumptions, the Kruskal–Wallis ANOVA was used for multiple comparisons and the Dunn's test was used *post hoc*. Data are presented as (mean ± SD). For all statistical tests, the level of significance was set at $P \leq 0.05$.

Results

In vitro SCF uses a nuclease in the luminal fluid that digests fully condensed sperm DNA

In our previous studies analyzing *in vitro* SCF, we routinely found that vas deferens sperm DNA was degraded to much smaller fragments than epididymal sperm DNA (Yamauchi *et al.*, 2007b). This was confusing as this degradation was far beyond the TLR limited digestion that was present in epididymal sperm, but the chromatin structure is similar in both. We had also shown that the vas deferens luminal fluid contained much more nuclease activity than that of the epididymis (Gawecka *et al.*, 2015). We suspected that this nuclease retained some activity even in the presence of 0.5% SDS used for the digestion of sperm for PFGE. We recently demonstrated that the luminal nuclease that digests DNA in SCF is active in SDS for a short time (Szczygieł *et al.*, 2022). These experiments were reproduced in a condensed form, here, for clarity. Epididymal luminal fluid incubated with Mn^{2+} then plugged in low melting agarose for PFGE and digested with SDS and DTT (digestion buffer) had DNA fragmented to toroid-sized lengths (25–50 kb, Supplementary Fig. S1, lane 2). When epididymal sperm were centrifuged and suspended in vas deferens luminal fluid, the digestion was far greater (Supplementary Fig. S1, lane 3), similar to that of vas deferens sperm (Supplementary Fig. S1, lane 9) because the vas deferens has a greater concentration of the nuclease (Gawecka, 2015). Vas deferens sperm in the presence of epididymal luminal fluid were digested less (Supplementary Fig. S1, lane 10). Incubation in SDS prior to Mn^{2+} addition inhibits nuclease digestion in both epididymal and vas deferens sperm (Supplementary Fig. S1, lanes 4 and 11), as does EDTA pretreatment (Supplementary Fig. S1, lanes 5 and 12). When sperm were incubated with Mn^{2+} then with EDTA, the digestion was limited to toroid-sized fragments in both epididymal (Supplementary Fig. S1, lane 6) and vas deferens sperm (Supplementary Fig. S1, lane 13). These data are consistent with our findings that nuclease digestion of the sperm DNA is limited to the TLRs when the chromatin is still condensed, but can further digest the DNA when SDS and DTT in the digestion buffer remove the protamines that normally protect the DNA from nuclease digestion. For all the experiments in this work, we used the conditions shown in Supplementary Fig. S1, lanes 6 and 13: namely treatment with Mn^{2+} then complete cessation of SCF with 50 mM EDTA for 30 min. These data demonstrate that the luminal nuclease that causes *in vitro* SCF is active in SDS for a short time and can be inhibited completely by EDTA treatment. They also demonstrate that when SCF activity is limited to fully condensed sperm (e.g. before SDS and DTT removal of protamines) the digestion is limited to TLRs.

We next conducted neutral Comet assays, which measure only DSB, to test whether the DNA breaks observed in the pulsed-field gels could be quantified at the single-cell level. OTM is essentially a measure of how much DNA escapes the nucleus, and has been chosen as an indicator of the amount of DNA breaks present in a specific cell (Langie *et al.*, 2015; Simon *et al.*, 2017). For neutral Comet controls, OTM values (mean ± SD) were 10.22 ± 14.36 and 12.58 ± 18.77, for cauda epididymis and vas deferens sperm, respectively. After 30-min incubation in Mn^{2+} followed by 30-min EDTA incubation, OTM were 45.41 ± 20.92 and 60.11 ± 22.45, respectively, for cauda epididymis and vas deferens, representing a statistically significant increase in both cases ($P < 0.001$; Supplementary Fig. S2). The increase caused by SCF on the epididymis sperm was 4.44-fold with respect to the control, while in vas deferens sperm there was 4.78-fold increase after SCF, compared to the control. Significant differences were found between epididymis sperm SCF and vas deferens sperm SCF ($P < 0.001$). Thus, our Comet assay data matched our PFGE findings.

Our model for SCF hypothesizes that the luminal nuclease digests sperm DNA *in situ* when the chromatin is fully compact, by digesting the TLRs that connect one protamine toroid to the other. To test this, we incubated epididymal and vas deferens sperm with EDTA (control) or Mn^{2+} and then EDTA (SCF) and analyzed the chromatin by thin-section transmission electron microscopy. The sperm

chromatin remained highly electron dense in untreated, control and SCF samples (Fig. 1).

Taken together, these data confirm our hypothesis that SCF can digest fully condensed sperm chromatin and that the digestion does not grossly disrupt the chromatin structure.

Vasectomy leads to *in vivo* SCF-like DNA breaks that are increased upon incubation in Mn^{2+}

Vasectomy causes SCF DNA breaks in cauda epididymis and vas deferens sperm

In all of our previous research on SCF to date, we have activated SCF *in vitro* by incubating sperm with Mn^{2+}. We hypothesized that SCF was an early part of the mechanism that normally functions to digest sperm DNA when spermatozoa are degraded *in vivo*. Vasectomy creates the need to remove sperm that build up at the site of the vas deferens excision, so we tested whether these sperm have DNA degradation consistent with SCF. Mice were vasectomized distally to the epididymis to ensure some vas deferens remained (Supplementary Fig. S3), and sperm were isolated from the cauda epididymis and the vas deferens remnants at 1, 2 and 3 weeks after vasectomy. We quantified the percentage of toroid-sized fragmented DNA (15–145 kb) in vasectomized and mock surgery controls by PFGE (Fig. 2A). Mock surgery induced a low level of DNA breaks. Vasectomized mice showed an increase in SCF-like breaks in sperm of both the cauda epididymis and the vas deferens gradually over the 3 weeks, although the latter had a much higher percentage of breaks. For example, sperm from vas deferens 3 weeks after vasectomy had a 7.1-fold increase in the percentage of toroid-sized DNA fragments compared to untreated controls (4.9 ± 1.15 versus 34.74 ± 16.17). These data suggest that vasectomy induces SCF-like degradation of mouse sperm DNA.

We next quantified the sperm DNA DSBs at the single-sperm level using the neutral Comet assay, which mirrored our PFGE data (Fig. 2B). The neutral Comet assay showed a similar pattern of DNA degradation as PFGE, but with greater sensitivity. Vasectomy caused more than a 6-fold increase in DNA breaks in both epididymal and vas deferens sperm at 3 weeks. Mock surgery induced a small, but non-significant increase in breaks. No increase was observed between control (no treatment) and mock for any time point ($P > 0.05$), but differences were observed between control and vasectomized mice for all time points ($P < 0.0001$).

These data demonstrate that vasectomy induces SCF-like breaks in mouse spermatozoa, *in vivo*.

Surgery causes collateral single-stranded DNA breaks, which are reduced after 3 weeks of recovery

We also performed alkaline Comet assays, which measure single- and double-stranded DNA breaks, on all samples and noticed that while mock surgery does not increase DSBs (Fig. 2), it does present an

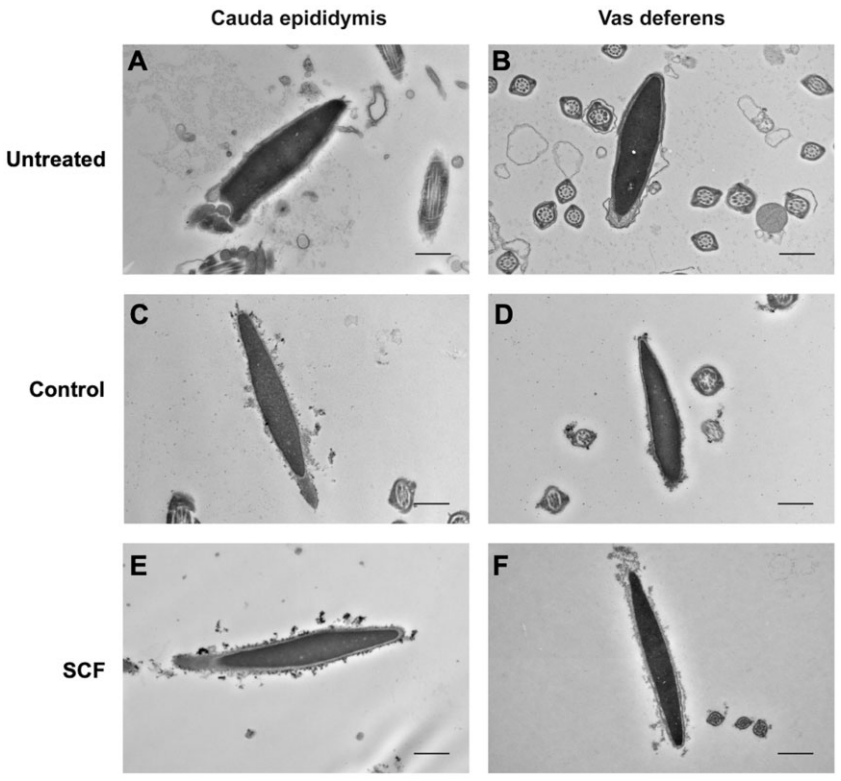

Figure 1. Sperm chromatin remains condensed after sperm chromatin fragmentation in mice. Transmission electron microscope images showed no differences in sperm chromatin condensation between (**A, B**) 0.25% Triton-X100 for 60 min, (**C, D**) 0.25% Triton-X100 for 30 min + 100 mM EDTA for 30 min and (**E, F**) 10 mM Mn^{2+} in 0.25% Triton-X100 for 30 min + 100 mM EDTA for 30 min. A, C and E correspond to cauda epididymis sperm and B, D and F are vas deferens sperm. Bars indicate 800 nm.

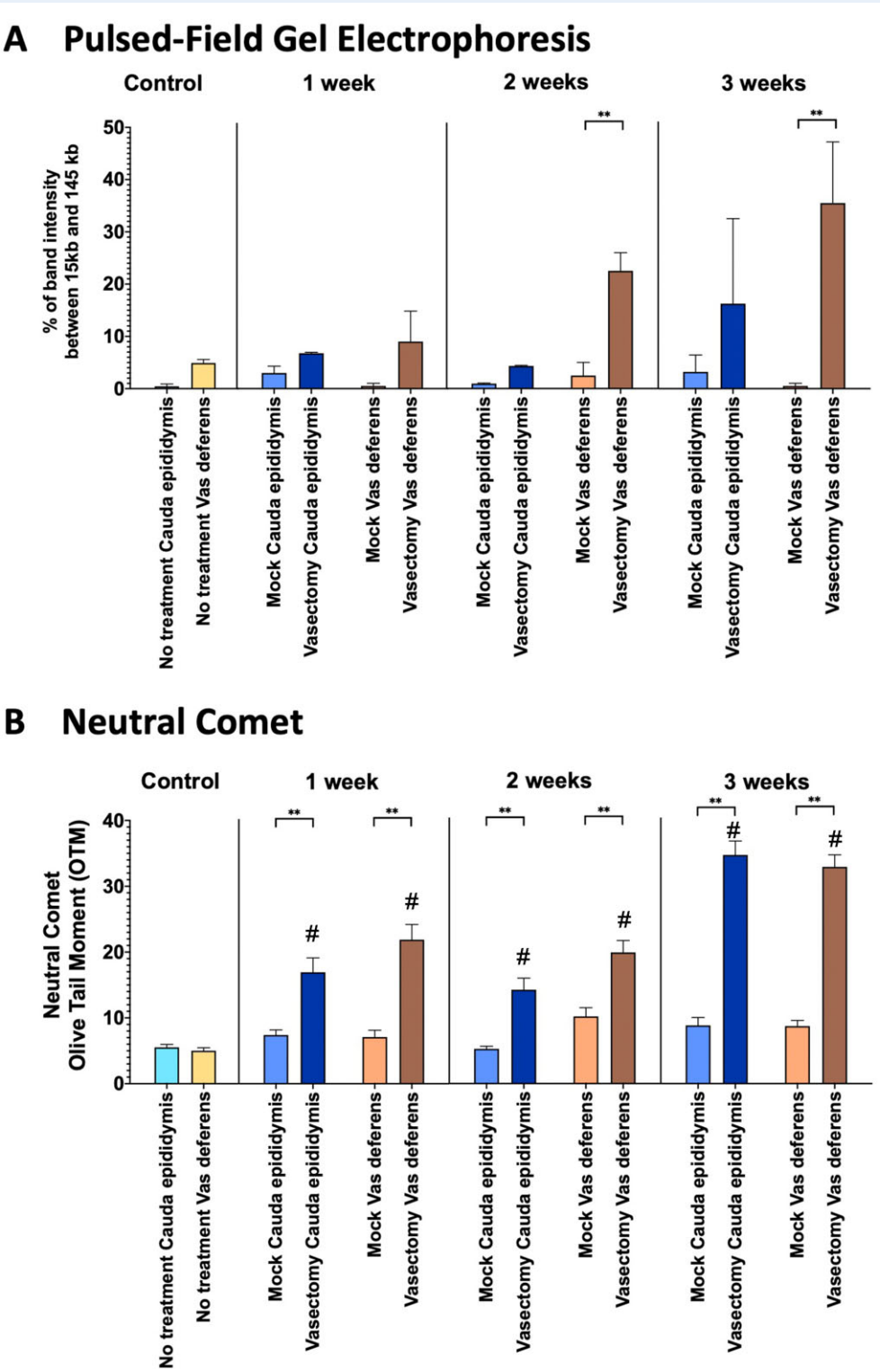

Figure 2. Double-stranded DNA damage increases after vasectomy in mice, for up to 3 weeks. Mice were vasectomized or underwent mock surgery, and sperm double-stranded DNA breaks were analyzed by pulsed-field gel electrophoresis (**A**) and the neutral Comet assay (**B**) after 1, 2 and 3 weeks. (A) Percentage of the DNA fragments sized between 15 and 145 kb, indicating the toroid-sized fragments caused by SCF mechanism. (B) Neutral Comet olive tail moment DNA fragmentation data at single-sperm level. #Statistically significant differences compared to the respective non-treated control (cauda epididymis or vas deferens; $P < 0.001$; Kruskal–Wallis ANOVA using Dunn's test as *post hoc*). **Statistically significant differences between vasectomy and mock samples ($P < 0.01$; Kruskal–Wallis ANOVA using Dunn's test as *post hoc*). The total sample size is n = 21, divided into n = 3 for control, and n = 3 for mock and n = 3 for vasectomy for each time point.

increase in single-stranded DNA breaks (SDBs) compared to untreated samples ($P < 0.01$; Supplementary Fig. S4). Vasectomy also showed a similar increase as mock, although in some cases, SDB values were increased ($P < 0.01$). At 1 and 2 weeks postsurgery, the number of SDBs rose in both vasectomized and mock surgery mice, although they were slightly higher than those in the mock surgery mice, except for 1 week in the epididymis. By 3 weeks postsurgery, however, the number of SDBs decreased compared to 2 weeks postsurgery. While the SDBs were still higher than controls for epididymal sperm ($P < 0.01$), in both mock and vasectomized vas deferens the sperm SDBs were not significantly different from controls ($P > 0.05$; Supplementary Fig. S4).

These data suggest that surgery, not vasectomy *per se*, causes trauma to the sperm cell that temporarily increases SDBs.

The in vitro *SCF mechanism remains active in vasectomized mice*

The hypothesis that we are testing in this study is that the same mechanism that causes SCF *in vitro* (Figs 1 and 2) is responsible for the DSBs in sperm after vasectomy (Fig. 2). We therefore tested whether *in vitro* SCF was still active in vasectomized mice. We incubated cauda epididymis and vas deferens sperm from vasectomized mice with $MnCl_2$ then EDTA to induce SCF and analyzed the DNA fragmentation by PFGE and the neutral Comet assay (Supplementary Fig. S5). Both assays showed that the *in vitro* SCF mechanism is active in vasectomized mice. Interestingly, the Comet assay exhibited a clear, statistically significant decrease in *in vitro* SCF at 2 and 3 weeks after vasectomy (Supplementary Fig. S5B).

Caput epididymis sperm are not affected by the *in vivo* SCF-like mechanism

Taking into account that SCF relies on a nuclease present in vas deferens fluid, we hypothesized that sperm from caput epididymis would be much less affected by SCF initiated in response to vasectomy than cauda epididymal sperm, since the former are much farther away from the source of the vas deferens nuclease. We tested this by comparing the response of cauda and caput sperm to vasectomy.

The luminal fluid of the caput epididymis contains many different types of cells in addition to sperm. In order to more specifically identify the sperm cells, we took advantage of the fact that sperm chromatin condensation renders sperm nuclei much less susceptible to disruption than somatic cells. We lysed the somatic cells with detergent that did not affect sperm nuclei and showed that this decreased the contamination from somatic cells (Supplementary Fig. S6). We next used this modified method to quantitate DSBs in caput and cauda epididymis sperm and vas deferens sperm from the same animal. The number of sperm in the caput epididymis was too low for PFGE analysis, but there was enough for the neutral Comet assay. Supplementary Fig. S7 shows neutral Comet assay OTM results for each mock and vasectomized individual mouse. There were no increases in DSBs for up to 3 weeks after vasectomy in the caput epididymal sperm ($P > 0.05$), while there were significant increases in DSBs for in both the cauda epididymal and vas deferens sperm in the same mice ($P < 0.05$), as seen above. No differences were found for caput epididymis between controls, mock and vasectomy ($P > 0.05$). Vas deferens presented statistically significant differences between mock and vasectomy at 2- and 3-week postvasectomy ($P < 0.05$).

Vasectomy causes cell death in both epididymal and vas deferens sperm

After elucidating that an SCF-like mechanism relying on a nuclease would be responsible for causing DNA breaks in sperm after vasectomy, starting at the vas deferens and affecting cauda epididymis, we tested whether cell death is also concomitant with this mechanism.

Figure 3 shows sperm viability for sperm from mock and vasectomized mice. We have found that vas deferens sperm viability was significantly reduced at 2 and 3 weeks after vasectomy ($P < 0.05$). Although cauda epididymis sperm viability was also reduced at these time points ($P < 0.05$), the percentage of dead sperm was lower than for vas deferens. Finally, caput epididymis only presented a reduction of sperm viability 3 weeks after vasectomy ($P < 0.05$).

Discussion

The evidence presented in this work supports a model that a mechanism by which sperm DNA is degraded into toroid-sized fragments *in vitro*, i.e. SCF, also functions *in vivo* after vasectomy in mice. The SCF is a mechanism that we have described *in vitro* in which a nuclease in the luminal fluid of the vas deferens initiates the cleavage of sperm chromatin at the TLRs (Yamauchi *et al.*, 2007a, 2009; Gawecka *et al.*, 2013, 2015). We found that the same pattern of DNA degradation occurs in sperm *in vitro* after vasectomy. In our previous publications, the luminal nuclease had to be activated with Mn^{2+} to digest the sperm DNA *in vitro*, but with vasectomy, the nuclease was activated *in vivo* without additional Mn^{2+} suggesting that, in vasectomy, SCF is activated by an endogenous mechanism. This work supports our hypothesis that SCF is an apoptotic-like mechanism that is activated to functionally disrupt the sperm chromatin, thereby preventing any sperm with potentially damaged DNA from fertilizing an embryo (Ward and Ward, 2004).

SCF can fragment fully condensed sperm chromatin

One potential barrier for nucleases to digest the fully condensed DNA in mature sperm chromatin is that accessibility to DNA is much more restricted in sperm than it is in somatic cells. Early thin-section electron microscopy studies revealed that sperm chromatin is almost completely electron dense (Wolff and Schill, 1975) (Fig. 1A and B), revealing no visible chromatin structure. Protamines protect DNA from complete nuclease digestion because of this tight condensation (Sotolongo *et al.*, 2003). However, our previously published data indicate that there are foci in the fully condensed sperm chromatin that are susceptible to external nucleases (Sotolongo *et al.*, 2003; Ward, 2010). Here, we demonstrated that when sperm DNA is fragmented by SCF *in vitro*, the sperm chromatin remains fully condensed (Fig. 1E and F). We previously proposed a model that protamine toroids are stacked (Fig. 4A). Although we have never previously depicted how we thought the larger chromatin fibers compacted, Fig. 4B depicts our proposed arrangement. While this model is not derived from the data in the present work, we show it to illustrate how we think the nuclease might digest the sperm TLRs without disrupting the overall packaging. Two aspects of this hypothesized model may work to keep the chromatin compact when the TLRs are digested by SCF in

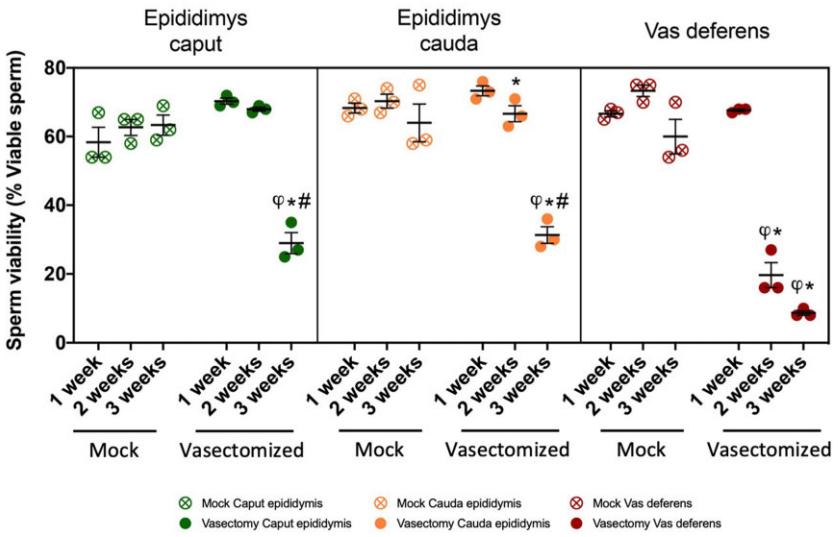

Figure 3. Viability of sperm from caput epididymis, cauda epididymis and vas deferens from three mock and three vasectomized mice, analyzed separately. *Statistically significant differences compared to 1 week after surgery (Kruskal–Wallis ANOVA using Dunn's test as *post hoc*). #Statistically significant differences compared to 2 weeks after vasectomy (Kruskal–Wallis ANOVA using Dunn's test as *post hoc*). ϕStatistically significant differences compared to the corresponding mock (Kruskal–Wallis ANOVA using Dunn's test as *post hoc*). The total sample size is n = 18, divided into n = 3 for mock and n = 3 for vasectomy for each time point.

vasectomized mice. First, we propose that the protamine toroids are bound by Van der Waals forces, tightly compacting the DNA. Second, we previously demonstrated that even when the TLRs are digested by SCF, much of the DNA remains associated with the nuclear matrix. Remarkably, we showed that DNA breaks caused in SCF remain attached to the nuclear matrix, and this might also contribute to maintaining the nuclear structure (Ribas-Maynou *et al.*, 2014).

Our model also suggests a possible structural access for nucleases to the TLRs in compact sperm chromatin. Because toroids are round (Allen *et al.*, 1992; Hud *et al.*, 1993), we suggest that the most dense configuration possible would be a hexagonal array of chromatin fibers, as shown by the hypothetical model in Fig. 4B. This would result in two possible channels, intra-toroidal channels formed from the holes in the centers of the protamine toroids, and inter-toroidal channels formed at the conjunction of the protamine toroid fibers. We would not expect the intra-toroidal channels to provide access to the TLRs. However, the existence of inter-toroidal channels would provide access for external proteins to the TLFs in compact chromatin. While we do not yet have strong evidence for either the stacking of protamine toroids (Fig. 4A) or the tightly packed array of fibers shown in Fig. 4B, these are, in our view, the most compact structures that a series of toroids could attain, and even in this model, a nuclease would have access to the nuclease-sensitive TLRs. Finally, in this model, digestion of the TLRs by a nuclease would not cause the sperm chromatin to decondense since the protamine toroids are still compacted by Van der Waals forces and possibly by interfiber disulfide crosslinks, plus the possible retention of TLR-digested DNA on the nuclear matrix. If TLRs are also the functional sites of DNA replication, as we have proposed (Shaman *et al.*, 2007; Yamauchi *et al.*, 2007a), this would also allow the newly formed embryo to access DNA replication origins in sperm DNA to reorganize the paternal genome, emphasizing the first functional aspect of paternal DNA replication.

SCF degrades sperm DNA *in vivo* after vasectomy

The analysis of mouse sperm retrieved after vasectomy showed an increased presence of DNA breaks that led to toroid-sized fragments. This suggests the positioning of the DSBs in the TLRs, suggesting the presence of an SCF-like mechanism *in vivo*. Our data also support a model for SCF, which is initiated by a nuclease that is in the vas deferens luminal fluid. We previously demonstrated that the luminal fluid in the vas deferens has a much higher capacity to support SCF *in vitro* (Gawecka *et al.*, 2015). We hypothesize that the lower levels of SCF in the cauda epididymis result from the vas deferens nuclease diffusing into the end of the epididymis when the vas deferens tubule is truncated. In the present work, we showed that, after vasectomy, the caput epididymis sperm, which is physically much more distal from the vas deferens than the cauda epididymis, does not undergo DNA fragmentation, supporting this model.

SCF may be part of a mechanism to degrade accumulated sperm after vasectomy

Vasectomy is a procedure that drastically interrupts sperm ejaculation through truncation of the vas deferens, leading to an obstructive azoospermia. Because the testis is unaffected by vasectomy, the sperm that continue to be produced must be degraded, reabsorbed or disintegrated. The fate of sperm after vasectomy has been the subject of

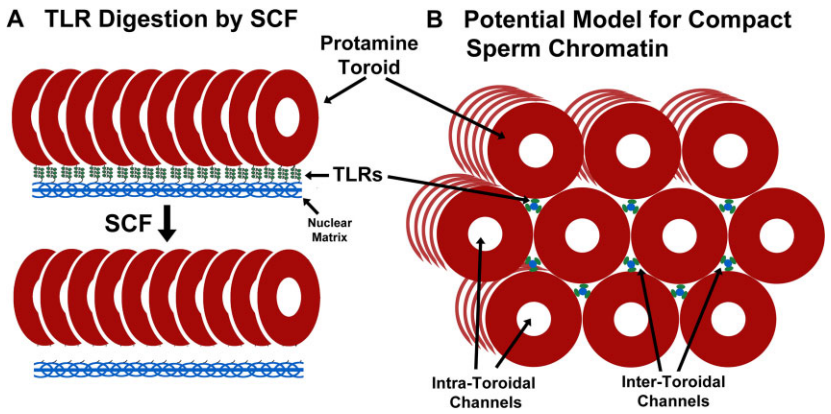

Figure 4. Toroid loop model for sperm chromatin. (**A**) We have proposed a model for sperm chromatin in which each protamine toroid is one DNA loop domain attached at their bases to a sperm nuclear matrix (Ward, 2010). The sperm chromatin fragmentation (SCF) causes DNA breaks at the toroid linker regions (TLRs). (**B**) A possible structure for how protamine toroid fibers might be compact. The model results in two channels that might provide proteins with access to the condensed sperm chromatin. Intra-toroidal channels might result from the center holes of toroids aligning. Inter-toroidal channels would result from the conjunction of cylindrical protamine toroid fibers compacting. We would expect TLRs to be located in inter-toroidal channels.

many studies. Most vasectomized men develop antisperm antibodies within a year of surgery (Alexander and Anderson, 1979). The appearance of sperm granulomas at the site of the vasectomy weeks after vas deferens obstruction is a likely mechanism through which sperm are eliminated (Nashan *et al.*, 1990; Jessop and Ladds, 1995; McDonald, 2000; Ma *et al.*, 2016), compensating for the fact that testis continues producing sperm (Peng *et al.*, 2011; Xiang *et al.*, 2013). Granulomas consist of a central mass of degenerating sperm, surrounded by macrophages and lymphocyte-rich vascular tissue (McDonald, 2000). They are observed in sheep, hamster and mouse, amongst others, weeks after the surgical procedure (Nashan *et al.*, 1990; Sun *et al.*, 1992; Jessop and Ladds, 1995). In some species, the epididymis becomes atrophied while in other animal models, such as the rabbit, the epididymis is maintained thanks to its ability to distend. In rabbits, sperm that are closer to the ligation site are dead and decapitated, but sperm counts are overall maintained after vasectomy (Wen *et al.*, 1994; Jones, 2004). In humans, some patients who had vasectomy reversal years after vasectomy became fertile, and both normal sperm and sperm fragments (i.e. broken heads) were found in their vas deferens fluids at the time of reversal surgery, indicating that testes maintain their production of sperm for a long time after vasectomy (Wen *et al.*, 1999; Kolettis *et al.*, 2006; Smith *et al.*, 2014).

The SCF-like mechanism activated in vas deferens presented here may contribute to the degradation of DNA from those sperm that need to be eliminated when ejaculation is no longer possible. The presence of DNA damage in sperm from vasectomized males has previously been observed in humans (Wen *et al.*, 1999; Ramos *et al.*, 2004; O'Neill *et al.*, 2007). A study conducted in vasectomized mice identified an increase of TUNEL-positive spermatids, but not in elongated spermatids, after 30 days (Liu *et al.*, 2014). Our PFGE experiments in combination with the neutral Comet assay confirmed that the DNA breaks are mainly localized in the TLRs, thus advocating for the SCF mechanism to be active in these sperm. In fact, incubations of the cauda epididymis and vas deferens sperm from vasectomized mice in Mn^{2+} led to even more DNA damage, reaching the levels found after 3 weeks of vasectomy (Supplementary Fig. S5), suggesting that the SCF mechanism is still active for up to 3 weeks after this surgical procedure.

Vasectomy surgery induces other types of DNA damage

While SCF is activated in sperm DNA after vasectomy, our results also demonstrate that SDBs appear in sperm DNA, but these do not persist for 3 weeks. In this case, the SDBs are induced by mock surgery to similar extents as vasectomy. This DNA damage may be caused by other mechanisms such as oxidative stress. This result is related to a study conducted with unilateral vasectomy in rats, where the authors demonstrated that vasectomy may induce oxidative stress in the testis (Liu *et al.*, 2014). Increased oxidative stress levels are known to lead to protein modifications, lipid peroxidation and DNA base modifications (Drevet and Aitken, 2019; Aitken *et al.*, 2022). Ultimately these alterations cause DNA damage and cell death, features that are observed in sperm from vasectomized mice.

Conclusion

In conclusion, the SCF mechanism is part of the elimination mechanism that sperm cells suffer after vasectomy, through which the DNA is cleaved into loop-sized fragments, contributing to the degradation of accumulated sperm.

Supplementary data

Supplementary data are available at *Molecular Human Reproduction* online.

Data availability

Databases obtained during the current study are available from the corresponding author on reasonable request.

Authors' roles

Conceptualization: J.R.-M., H.N. and W.S.W.; Methodology: J.R.-M., H.N., H.W., R.V. and W.S.W. Formal analysis and investigation: J.R.-M. and W.S.W.; Writing—original draft preparation: J.R.-M. and W.S.W.; Writing—review and editing: J.R.-M., M.Y. and W.S.W.; Funding acquisition: J.R.-M. and W.S.W.; Supervision: W.S.W. All the authors have read and agreed to the published version of the manuscript.

Funding

This research was supported by the European Union's Horizon 2020 Research and Innovation Scheme under the Marie Skłodowska-Curie grant agreement No. 801342 (Tecniospring INDUSTRY; TECSPR-19-1-0003), to J.R.-M.; the NIH, grant number GM123048 to W.S.W.; the Catalan Agency for Management of University and Research Grants, Regional Government of Catalonia, Spain (2017-SGR-1229); the Catalan Institution for Research and Advanced Studies (ICREA); and La Marató de TV3 Foundation (214/857-202039).

Conflict of interest

The authors declare that they have no conflict of interest.

References

Abdelmassih V, Balmaceda JP, Tesarik J, Abdelmassih R, Nagy ZP. Relationship between time period after vasectomy and the reproductive capacity of sperm obtained by epididymal aspiration. *Hum Reprod* 2002;**17**:736–740.

Aitken RJ, Drevet JR, Moazamian A, Gharagozloo P. Male infertility and oxidative stress: a focus on the underlying mechanisms. *Antioxidants* 2022;**11**:306.

Alexander NJ, Anderson DJ. Vasectomy: consequences of autoimmunity to sperm antigens. *Fertil Steril* 1979;**32**:253–260.

Allen MJ, Hud NV, Balooch M, Tench RJ, Siekhaus WJ, Balhorn R. Tip-radius-induced artifacts in AFM images of protamine-complexed DNA fibers. *Ultramicroscopy* 1992;**42–44**:1095–1100.

Bedford JM, Zelikovsky G. Viability of spermatozoa in the human ejaculate after vasectomy. *Fertil Steril* 1979;**32**:460–463.

Belleannée C, Légaré C, Calvo É, Thimon V, Sullivan R. microRNA signature is altered in both human epididymis and seminal microvesicles following vasectomy. *Hum Reprod* 2013;**28**:1455–1467.

Boaz SM, Dominguez K, Shaman JA, Ward WS. Mouse spermatozoa contain a nuclease that is activated by pretreatment with EGTA and subsequent calcium incubation. *J Cell Biochem* 2008;**103**:1636–1645.

Borges E, Braga DPdAF, Iaconelli A, Setti AS. The obstructive interval predicts pregnancy rates in post-vasectomy patients undergoing ICSI with surgical sperm retrieval. *Reprod Biomed Online* 2019;**39**:134–140.

Borges E, Rossi-Ferragut LM, Pasqualotto FF, Rocha CC, Iaconelli A. Different intervals between vasectomy and sperm retrieval interfere in the reproductive capacity from vasectomized men. *J Assist Reprod Genet* 2003;**20**:33–37.

Castro LS, Siqueira AFP, Hamilton TRS, Mendes CM, Visintin JA, Assumpção MEOA. Effect of bovine sperm chromatin integrity evaluated using three different methods on in vitro fertility. *Theriogenology* 2018;**107**:142–148.

Crespo F, Wilson R, Díaz-Jimenez M, Consuegra C, Dorado J, Barrado BG, Gosálvez J, Smit RL, Hidalgo M, Johnston S. Effect of season on individual stallion semen characteristics. *Anim Reprod Sci* 2020;**223**:106641.

Doiron K, Légaré C, Saez F, Sullivan R. Effect of vasectomy on gene expression in the epididymis of cynomolgus monkey. *Biol Reprod* 2003;**68**:781–788.

Drevet JR, Aitken RJ. Oxidative damage to sperm DNA: attack and defense. *Adv Exp Med Biol* 2019;**1166**:107–117.

Esteves SC, López-Fernández C, Martínez MG, Silva EA, Gosálvez J. Reliability of the sperm chromatin dispersion assay to evaluate sperm deoxyribonucleic acid damage in men with infertility. *Fertil Steril* 2022;**117**:64–73.

Gawecka JE, Boaz S, Kasperson K, Nguyen H, Evenson DP, Ward WS. Luminal fluid of epididymis and vas deferens contributes to sperm chromatin fragmentation. *Hum Reprod* 2015;**30**:2725–2736.

Gawecka JE, Marh J, Ortega M, Yamauchi Y, Ward MA, Ward WS. Mouse zygotes respond to severe sperm DNA damage by delaying paternal DNA replication and embryonic development. *PLoS One* 2013;**8**:e56385.

Gong J, Traganos F, Darzynkiewicz Z. A selective procedure for DNA extraction from apoptotic cells applicable for gel electrophoresis and flow cytometry. *Anal Biochem* 1994;**218**:314–319.

Hammoud I, Bailly M, Bergere M, Wainer R, Izard V, Vialard F, Selva J, Boitrelle F. Testicular spermatozoa are of better quality than epididymal spermatozoa in patients with obstructive azoospermia. *Urology* 2017;**103**:106–111.

Hammoud SS, Nix DA, Zhang H, Purwar J, Carrell DT, Cairns BR. Distinctive chromatin in human sperm packages genes for embryo development. *Nature* 2009;**460**:473–478.

Hud NV, Allen MJ, Downing KH, Lee J, Balhorn R. Identification of the elemental packing unit of DNA in mammalian sperm cells by atomic force microscopy. *Biochem Biophys Res Commun* 1993;**193**:1347–1354.

Hud NV, Downing KH, Balhorn R. A constant radius of curvature model for the organization of DNA in toroidal condensates. *Proc Natl Acad Sci U S A* 1995;**92**:3581–3585.

Jessop TS, Ladds PW. The immunopathology of unilateral vasectomy in the ram. *Vet Immunol Immunopathol* 1995;**47**:123–133.

Jones R. Sperm survival versus degradation in the Mammalian epididymis: a hypothesis. *Biol Reprod* 2004;**71**:1405–1411.

Khaira HS, Schuster TG, Zhang WX, Dunn R, Smith GD, Ohl DA. Epididymal obstruction results in isolated sperm heads in post-vasectomy rats. *Int J Androl* 2007;**30**:56–60.

Kolettis PN, Burns JR, Nangia AK, Sandlow JI. Outcomes for vasovasostomy performed when only sperm parts are present in the vasal fluid. *J Androl* 2006;**27**:565–567.

Langie SAS, Azqueta A, Collins AR. The comet assay: past, present, and future. *Front Genet* 2015;**6**:266.

Légaré C, Verville N, Sullivan R. Vasectomy influences expression of HE1 but not HE2 and HE5 genes in human epididymis. *J Androl* 2004;**25**:30–43.

Liu J, Rong CT, Li Y, Liu XX, Wang WT, Li N. Vasectomy induces oxidative stress and up-regulates the expression of peroxiredoxins in mouse testis in short and early periods after surgery. *J Urol* 2014;**191**:1920–1926.

Ma L, Guo Y, Yuan Y, Li YG, Deng XZ, Yang ZW. Morphometric study of the testis and reproductive tract (including sperm granuloma) after vasectomy in mature rats. *Asian J Androl* 2016;**18**: 66–73.

McDonald SW. Cellular responses to vasectomy. *Int Rev Cytol* 2000; **199**:295–339.

Mendonça GA, Morandi R, Souza ET, Gaggini TS, Silva-Mendonça MCA, Antunes RC, Beletti ME. Isolation and identification of proteins from swine sperm chromatin and nuclear matrix. *Anim Reprod* 2017;**14**:418–428.

Mohar I, Szczygiel MA, Yanagimachi R, Ward WS. Sperm nuclear halos can transform into normal chromosomes after injection into oocytes. *Mol Reprod Dev* 2002;**62**:416–420.

Mudrak O, Tomilin N, Zalensky A. Chromosome architecture in the decondensing human sperm nucleus. *J Cell Sci* 2005;**118**: 4541–4550.

Nashan D, Cooper TG, Knuth UA, Schubeus P, Sorg C, Nieschlag E. Presence and distribution of leucocyte subsets in the murine epididymis after vasectomy. *Int J Androl* 1990;**13**:39–49.

O'Neill DA, McVicar CM, McClure N, Maxwell P, Cooke I, Pogue KM, Lewis SEM. Reduced sperm yield from testicular biopsies of vasectomized men is due to increased apoptosis. *Fertil Steril* 2007; **87**:834–841.

Peng B, Mao Y, Tang XF, Shang Y, Shen CY, Guo Y, Xiang Y, Yang ZW. Comparison of spermatogenic damage induced at 6 months after ligation of the vas deferens at proximal and distal locations in the rabbit. *Andrologia* 2011;**43**:129–138.

Peng B, Wang YP, Shang Y, Guo Y, Yang ZW. Effect of vasectomy via inguinal canal on spermatogenesis in rabbits. *Asian J Androl* 2008;**10**:486–493.

Peris-Frau P, Álvarez-Rodríguez M, Martín-Maestro A, Iniesta-Cuerda M, Sánchez-Ajofrín I, Garde JJ, Rodriguez-Martinez H, Soler AJ. Comparative evaluation of DNA integrity using sperm chromatin structure assay and Sperm-Ovis-Halomax during in vitro capacitation of cryopreserved ram spermatozoa. *Reprod Domest Anim* 2019;**54**(Suppl. 4):46–49.

Ramos L, de Boer P, Meuleman EJH, Braat DDM, Wetzels AMM. Chromatin condensation and DNA damage of human epididymal spermatozoa in obstructive azoospermia. *Reprod Biomed Online* 2004;**8**:392–397.

Ribas-Maynou J, Benet J. Single and double strand sperm DNA damage: different reproductive effects on male fertility. *Genes (Basel)* 2019;**10**:105–110.

Ribas-Maynou J, Gawecka JE, Benet J, Ward WS. Double-stranded DNA breaks hidden in the neutral Comet assay suggest a role of the sperm nuclear matrix in DNA integrity maintenance. *Mol Hum Reprod* 2014;**20**:330–340.

Ribas-Maynou J, Llavanera M, Mateo-Otero Y, Garcia-Bonavila E, Delgado-Bermúdez A, Yeste M. Direct but not indirect methods correlate the percentages of sperm with altered chromatin to the intensity of chromatin damage. *Front Vet Sci* 2021;**8**:719319.

Richardson DW, Aitken RJ, Loudon NB. The functional competence of human spermatozoa recovered after vasectomy. *J Reprod Fertil* 1984;**70**:575–579.

Samans B, Yang Y, Krebs S, Sarode GV, Blum H, Reichenbach M, Wolf E, Steger K, Dansranjavin T, Schagdarsurengin U. Uniformity of nucleosome preservation pattern in mammalian sperm and Its connection to repetitive DNA elements. *Dev Cell* 2014;**30**:23–35.

Shaman JA, Yamauchi Y, Ward WS. The sperm nuclear matrix is required for paternal DNA replication. *J Cell Biochem* 2007;**102**: 680–688.

Shiraishi K, Naito K, Yoshida KI. Vasectomy impairs spermatogenesis through germ cell apoptosis mediated by the p53-BAX pathway in rats. *J Urol* 2001;**166**:1565–1571.

Shiraishi K, Yoshida KI, Fujimiya T, Naito K. Activation of mitogen activated protein kinases and apoptosis of germ cells after vasectomy in the rat. *J Urol* 2002;**168**:1273–1278.

Simon L, Aston KI, Emery BR, Hotaling J, Carrell DT. Sperm DNA damage output parameters measured by the alkaline Comet assay and their importance. *Andrologia* 2017;**49**:e12608.

Smith RP, Khanna A, Kovac JR, Badhiwala N, Coward R, Lipshultz LI. The significance of sperm heads and tails within the vasal fluid during vasectomy reversal. *Indian J Urol* 2014;**30**:164–168.

Solovyan VT, Bezvenyuk ZA, Salminen A, Austin CA, Courtney MJ. The role of topoisomerase II in the excision of DNA loop domains during apoptosis. *J Biol Chem* 2002;**277**:21458–21467.

Sotolongo B, Huang TTF, Isenberger E, Ward WS. An endogenous nuclease in hamster, mouse, and human spermatozoa cleaves DNA into loop-sized fragments. *J Androl* 2005;**26**:272–280.

Sotolongo B, Lino E, Ward WS. Ability of hamster spermatozoa to digest their own DNA. *Biol Reprod* 2003;**69**:2029–2035.

Sun YB, Qiu Y, Wang ZX. Vasectomy and spermatic granuloma in hamsters. *Contraception* 1992;**45**:177–185.

Szczygieł H, Ung A, Nguyen H, Ward WS. Update on toroid linker model for sperm chromatin. In: Patuszak A, Hotaling J, Carrell D (eds). *Men's Reproductive and Sexual Health Throughout the Lifespan*. Cambridge, UK: Cambridge University Press, 2022.

Villani P, Eleuteri P, Grollino MG, Rescia M, Altavista P, Spanò M, Pacchierotti F, Cordelli E. Sperm DNA fragmentation induced by DNAse I and hydrogen peroxide: an in vitro comparative study among different mammalian species. *Reproduction* 2010;**140**:445–452.

Ward MA, Ward WS. A model for the function of sperm DNA degradation. *Reprod Fertil Dev* 2004;**16**:547–554.

Ward WS. Function of sperm chromatin structural elements in fertilization and development. *Mol Hum Reprod* 2010;**16**:30–36.

Wen R, Li S, Wang C, Wang Q, Li Q, Feng H, Jiang Y, Huang J. Analysis of spermatozoa from the proximal vas deferens of vasectomized men. *Int J Androl* 1994;**17**:181–185.

Wen RQ, Li SQ, Wang CX, Wang QH, Liu MY. Morphological changes of spermatozoa in proximal vas deferens after vasectomy. *Asian J Androl* 1999;**1**:61–65.

Wolff HH, Schill WB. Ultrastructural study of human sperm acrosome during acetic acid extraction of acrosin. *J Reprod Fertil* 1975; **42**:385–387.

Xiang Y, Luo P, Cao Y, Yang ZW. Long-term effect of vasectomy on spermatogenesis in men: a morphometric study. *Asian J Androl* 2013;**15**:434–436.

Yamauchi Y, Shaman JA, Boaz SM, Ward WS. Paternal pronuclear DNA degradation is functionally linked to DNA replication in mouse oocytes. *Biol Reprod* 2007a;**77**:407–415.

Yamauchi Y, Shaman JA, Ward WS. Topoisomerase II-mediated breaks in spermatozoa cause the specific degradation of paternal DNA in fertilized oocytes. *Biol Reprod* 2007b;**76**:666–672.

Yamauchi Y, Ward MA, Ward WS. Asynchronous DNA replication and origin licensing in the mouse one-cell embryo. *J Cell Biochem* 2009;**107**:214–223.